HYDRODYNAMICS AND HEAT TRANSFER IN CURVILINEAR CHANNELS OF RECTANGULAR CROSS SECTION

K. V. Dement'eva and I. Z. Aronov

UDC 536.242:532.542

Experimental results of a study of hydraulic resistance and heat transfer in helical channels of rectangular cross section for laminar and turbulent flows in the isothermal and nonisothermal regimes are given.

The motion of liquids and gases in helical channels of rectangular cross section is applied in heat-transfer apparatus used in various branches of technology. Results of experimental and theoretical studies in this area were given in several papers and refer mostly to flow and heat-transfer conditions in curvilinear helical channels of tetragonal cross section [1, 2] or in a rectangular slit [3], where the height significantly exceeds the width ($h \gg b$).

Curvilinear channels with a radial arrangement of 3 large dimension of the slit cross section with respect to the main axis ($b \gg h$) have so far not been considered from the point of view of flow and heat transfer. In these channels the action of centrifugal forces is more pronounced. Secondary flows generated in curvilinear flow enclose the whole cross section of the channel. This results in intensification of heat transfer with respect to that with curvilinear channels having different cross-sectional orientations with respect to the axis.

The present work is a study of flow and heat transfer in curvilinear channels for various orientations and cross-sectional shapes.

The experiments were performed on an experimental setup consisting of detachable curvilinear brass channels of thickness 2 mm, as well as on a test bench, where a steel heating boiler that provided curvilinear gas flow was constructed. Each operating channel is a helical heat exchanger with rectangular-slit cross sections, consisting of three full coils, and is adjacent to the exit and entrance of the curvilinear parts of the straight portions.

The gas guides in the heating boiler were structurally designed in the form of seven water-cooled steel disk panels, between which the combustion products passed in six parallel flows, performing an incomplete rotation around the axis. Geometric similarity with the model test channels was maintained in the construction of the gas guides.

The basic geometric characteristics of the channels are given in Table 1. Type I refers to models of channels and gas boilers having a radial location larger on the side of the slit cross section, and type II is characteristic of larger-side location parallel to the main axis of the channel (Fig. 1).

As the heat carrier in the experimental setup we used hot air having a temperature $T_0 = (323\text{-}723)\,^\circ K$ at the exit of the channel. The use of a blower allowed us to obtain air velocities in the test channel reaching 80 m/sec and Reynolds numbers $Re = (0.5\text{-}38)\cdot 10^3$.

The walls of the second, third, and fourth channels were cooled in a case with circulating water, while the first and sixth channels were provided individual cooling of the internal, front-end, and exterior walls. The measurement scheme consisted of determination of temperature, heat flow densities, pressure drops at the test portions, heat-carrier flow rates, and power inputs. The air temperatures at the input and output of channels and in the five cross sections of the air path, as well as the temperatures of the internal, front-end, and exterior walls, were measured in the same cross sections on the side of the air by nickel—chromium (diameter 0.5 and 0.2 mm) thermocouples. Data units were set up at the second, third, and fourth test channels, measuring the thermal flows at the internal, front-

Scientific-Research Institute of Sanitary Engineering, Equipment, and Construction, Kiev. Translated from Inzhenerno-Fizicheskii Zhurnal, Vol. 34, No. 6, pp. 994-1000, June, 1978. Original article submitted June 14, 1977.

 0022-0841/78/3406-0666$07.50

TABLE 1. Geometric and Relative Channel Sizes

Parameters	Type I					Type II
	1	2	3	4	5	6
Mean diameter of the bend D, mm	112	112	190	314	400	112
Width of transverse cross section b, mm	76,5	74	74	80	300	4,2
Height of transverse cross section h, mm	5,5	4,7	4,7	4,7	22	73
Equivalent diameter d_e, mm	10,3	9,4	9,4	9,4	44	8,4
Curvature parameter d_e/D	0,092	0,084	0,050	0,030	0,110	0,075
Form factor b/h	14	15,8	15,8	17	13,6	0,058

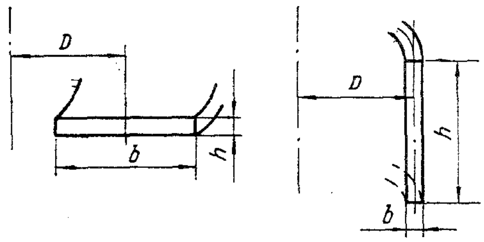

Type I Type II

Fig. 1. Construction scheme of models for curvilinear channels of rectangular cross section.

end, and exterior walls in each of the five cross sections. All thermocouples and heat-flow data units (HFDU) were connected to PP-63 potentiometers.

The air flow rate was measured by a chamber diaphragm and a DT-50 differential manometer, and the water flow was determined by bulk methods. The static pressures at all walls of the input and output channel cross sections were determined by the U-shaped manometers mentioned and by micromanometers. All measurements were performed under steady-state conditions.

The measurement and construction scheme of the experimental setup allowed us to determine the mean values of the hydraulic-resistance coefficient in the curvilinear portion of the channels. Sufficient length of the adjacent straight portions at each channel guaranteed hydrodynamic stabilization of flow in front of the input to the curvilinear portions. The experiments were performed for isothermal (293°K) and nonisothermal flows with heat flow densities of $(1-4)\cdot 10^4$ W/m^2.

The temperature and thermal flow changes at the walls allowed us to determine the heat-transfer coefficients averaged over the channel and the local heat-transfer coefficients in the separate cross sections.

The hydraulic-resistance coefficient ξ was determined from the Darcy–Weissbach equations. To determine the pressure loss in the curvilinear portion of the channel in the isothermal flow regime from the total pressure loss experimentally determined, the losses in the curvilinear portions were calculated using the equation for smooth channels in the turbulent regime.

In the case of nonisothermal motion, an additional pressure loss was included due to gas acceleration, which for the case of flow in a channel of constant cross section is equal to the kinetic energy difference at the initial and final cross sections.

The experimental results were first handled in the form of the dependence $\xi = f(\mathrm{Re})$ for each of the channels. A stratification of the experimental data was observed, depending on the curvature parameters d_e/D, higher ξ values being observed for channels with the largest curvature. Furthermore, enhanced Re numbers lead to lower ξ values. If in the turbulent regime the dependence $\xi = f(\mathrm{Re})$ is similar to the dependence for straight pipes and channels, an enhancement of the Re number in the laminar region is accompanied by a less intense lowering of the hydraulic resistance compared to the corresponding values in straight pipes and channels. The values of ξ_l and ξ_t for type-II channels seemed to be much lower than the

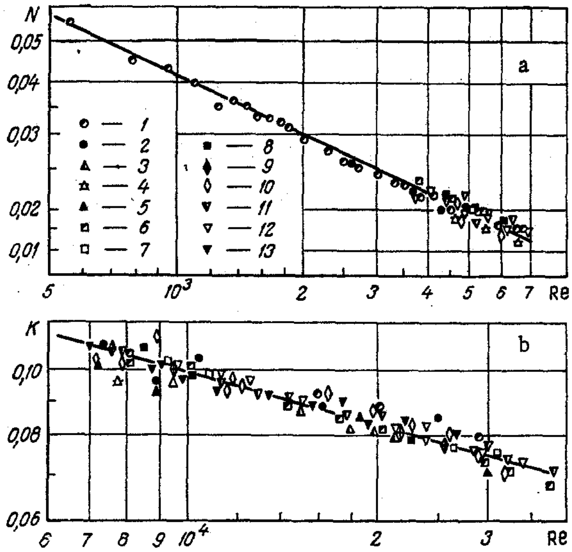

Fig. 2. Generalization of experimental data on hydraulic resistance: a) laminar regime; b) turbulent regime. Type I, d_e/D = 0.092; 1) isothermal regime; 2) T_0 = 473°K; d_e/D = 0.084; 3) isothermal regime; 4) 423°K; 5) 473°K; d_e/D = 0.05; 6) isothermal region; 7) 373°K; 8) 473°K; d_e/D = 0.03; 9) 323°K; 10) 373°K; type II for d_e/D = 0.075: 11) isothermal regime; 12) 373°K; 13) 473°K. $N = \xi/[1.97 + 49.1(d_e/D)^{1.32}(b/h)^{0.37}]$; $K = \xi/[0.316 + 865(d_e/D)^{1.32}(b/h)^{0.34}]$.

corresponding quantities for a type-I channel of equal curvature and insignificantly higher than ξl_{st} and ξt_{st} for straight pipes and channels. This is explained by the fact that in type-II channels the radial bends of the internal and exterior walls are close in magnitude, leading to a less significant effect of the centrifugal force on the motion of flow; moreover, in channels with h >> b, favorable conditions for generation of pair vortices are created only near planar walls; therefore, secondary flows cover only a small part and have little effect on the hydrodynamics and heat transfer.

The studies in the hydrodynamic region in curvilinear channels were used to obtain generalized equations taking into account changes in the form factor b/h. Figure 2a, b shows the experimental data on hydraulic resistance for curvilinear channels with any orientation of the rectangular cross section. The experimental data are approximated by the equations

$$\xi_L = \mathrm{Re}^{-0.46}\left[1.97 + 49.1\left(\frac{d_e}{D}\right)^{1.32}\left(\frac{b}{h}\right)^{0.37}\right] \quad \text{for} \quad \mathrm{Re} = (0.5-7)\cdot 10^3, \tag{1}$$

$$\xi_T = \mathrm{Re}^{-0.25}\left[0.316 + 8.65\left(\frac{d_e}{D}\right)^{1.32}\left(\frac{b}{h}\right)^{0.34}\right] \quad \text{for} \quad \mathrm{Re} = (7-38)\cdot 10^3. \tag{2}$$

It should be noted that in the limiting case d_e/D = 0, Eq. (1) acquires the form of the Blasius equation for straight pipes and channels. Thus, in the turbulent regime the enhanced hydraulic resistance in curvilinear channels is taken into account by the second term.

In studying heat transfer in curvilinear channels of rectangular cross section, provision was made for the determination of local and mean characteristics over the channel. Setting up HFDUs in type-I channels allowed us to obtain the local values of thermal flows in five cross sections along the operating portion at the internal, front-end, and exterior walls. The local values of α refer to the local kinetic temperature and were calculated with account taken of the thermal resistance due to the HFDUs [4].

Analysis of the α distribution showed that in the input channel for each wall $\alpha_{in} \simeq \alpha_{f-e} \approx \alpha_{ex}$; moving the heat carrier in the axial direction, the values of α_i drop and then reach constant values in the beginning or the middle of the second coil (with increasing Re numbers, the nonstabilized heat transfer is reduced for all channels). In achieving thermal stabilization for average Re numbers, the α values are distributed over the cross section

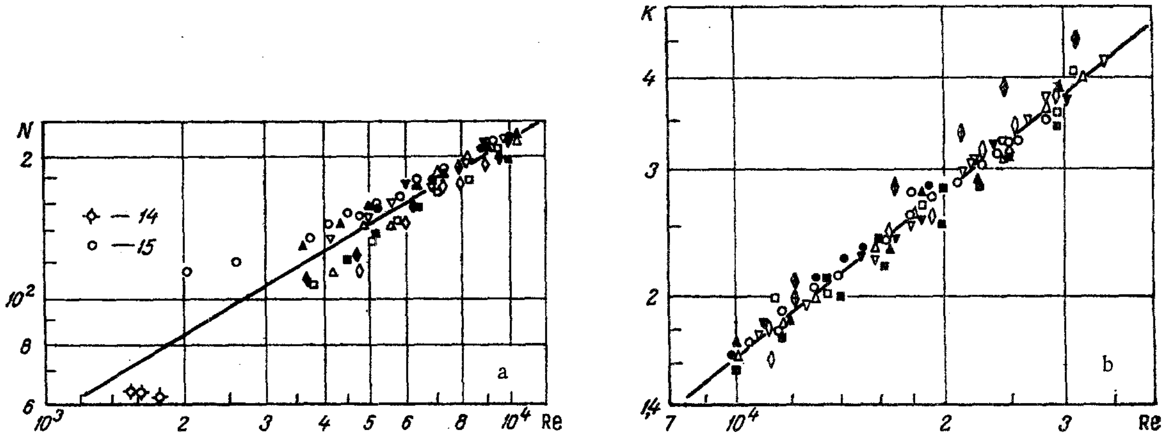

Fig. 3. Generalization of experimental heat-transfer data: a) laminar regime; b) turbulent: type-I for $d_e/D = 0.11$: 14) $T_0 = 1170°K$; $d_e/D = 0.092$; 15) 373°K. The remaining notation is the same as in Fig. 1. $N = Nu/Pr^{0.4}(1.5-0.5\theta)-[0.004 + 0.104\,(De \cdot d_e/D)^{0.13}]z$; $K = Nu \cdot 10^{-3}/Pr^{0.4}(1.5-0.5\theta)[0.021 + 0.077(d_e/D)^{1.22}(b/h)^{0.22}]$.

as follows: $\alpha_{f-e} > \alpha_{in} > \alpha_{ex}$. With increasing Re values, the values of α_{ex} approach those of α_{f-e}.

The local values of α_i obtained in the five cross sections of the channel were first determined along the channel for each wall separately by the equation $\bar{\alpha} = \frac{1}{x}\int_0^x \alpha_i dx_i$, and then for the channel as a whole. These quantities differed from those obtained by the balance method by 10-30%.

All experimental data on heat transfer were first handled in the form of the dependence $Nu/Pr^{0.4} = f(Re)$. The power of Re for all type-i channels equalled 0.58 in the laminar region and 0.8 in the turbulent one; for type-II channels it was 0.8 for all Re numbers investigated.

The heat-transfer intensity increases with enhanced curvature parameter d_e/D in type-I channels. If the dependence $Nu_{T_I}/Pr^{0.4}Re^{0.8} = f(d_e/D)$ was observed for the turbulent regime, then in the laminar regime the heat-transfer intensity depends also on the Dean number: $Nu_{l_I}/Pr^{0.4}Re^{0.58} = f(Ded_e/D)$. Obviously, the effect of mass forces is more significant in the laminar regime.

Similarly to the dependences characterizing the hydraulic resistance in a curvilinear type-II channel, the heat-transfer intensity differs also here insignificantly from that for straingt pipes and channels. Moreover, some enhanced heat transfer with enhanced temperature factor θ, noted earlier for straight pipes and channels [5], was noted in heat-transfer experiments during cooling of the heated air in all curvilinear channels of rectangular cross section [5].

The experimental heat-transfer data in curvilinear channels with arbitrary orientation of the rectangular cross section are shown in Fig. 3a. The experimental results in the laminar region are approximated by the equation

$$Nu_L = Pe^{0.58}Pr^{0.4}\,[0{,}004 + 0.104\,(Ded_e/D)^{0.13}]\,(1.5 - 0.5\Theta)z \tag{3}$$

$$\text{for}\quad Re = (3 - 10)\cdot 10^3 \ \text{and}\ De = 60 - 250.$$

Here the function z includes the effect of the geometric parameter b/h:

$$z = [0.035 + 0.654\,(Ded_e/D)^{0.053}](b/h)^{0.08-0.0018(Ded_e/D)^{0.59}}. \tag{4}$$

For type-II curvilinear channels with rectangular-slit cross sections the dependence $z = f(Ded_e/D)$ was calculated for $b/h = 0.0575$: for Ded_e/D = 61, 98, 146, 195, and 244 z equals 0.714, 0.744, 0.776, 0.800, and 0.824, respectively.

For b/h = 13-15 (type-I channels) z = 1; in this case Eq. (3) simplifies significantly and can be used to calculate heat transfer in type-I curvilinear channels.

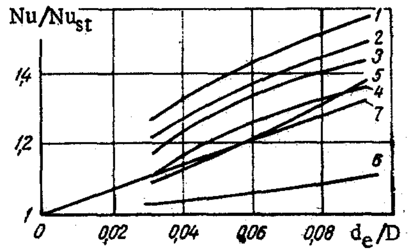

Fig. 4. The dependence $Nu/Nu_{st} = f(d_e/D)$: 1-4) calculated data in the laminar region by Eq. (6) for z = 1: 1) Re = 2500; 2) 4000; 3) 6000; 4) 10^4; 5, 6) calculated data in the turbulent region by Eq. (7) for Re > 10^4: 5) type-I channels; 6) type-II; 7) calculated data by Eq. (8).

The experimental heat-transfer data in the turbulent flow regime in curvilinear channels with arbitrary orientation of the rectangular cross section are described by the equation (see Fig. 3b)

$$Nu_T = Re^{0.8}Pr^{0.4}[0.021 + 0.0768(d_e/D)^{1.22}(b/h)^{0.22}](1.5 - 0.5\theta) \quad \text{for} \quad Re = (1 - 3.8)\cdot 10^4. \tag{5}$$

Thus, the enhanced heat-transfer intensity in the turbulent flow regime in curvilinear channels of rectangular cross section is taken into account by the second term in the square brackets. In the limiting case $d_e/D = 0$, Eq. (5) acquires a form characteristic of heat transfer in straight pipes and channels.

Equations (3) and (5) were reduced to the form

$$Nu_L/Nu_{st} = Re^{-0.22}[0.19 + 4.95(De\,d_e/D)^{0.13}]z, \tag{6}$$

$$Nu_T/Nu_{st} = 1 + 3.66(d_e/D)^{1.22}(b/h)^{0.22}, \tag{7}$$

where

$$Nu_{st} = 0.021Re^{0.8}Pr^{0.4}(1.5 - 0.5\theta) \quad \text{for} \quad Re > 2300.$$

Calculations by Eqs. (6) and (7) allowed us to draw conclusions on the enhancement of heat-transfer intensity in curvilinear channels of rectangular cross section in comparison with straight pipes and channels (Fig. 4). In type-I channels for z = 1 the heat-transfer intensification for the laminar regime is quite significant, particularly for small Re numbers, and reaches 40-55% at $d_e/D \approx 0.1$. With increasing Re, the values of Nu/Nu_{st} drop in the limit of the laminar regime (curves 1-4) and for Re ≈ 10^4 becomes comparable to Nu/Nu_{st} values in the turbulent flow regime (curve 5). In type-II channels (curve 6) the turbulent flow for b/h = 0.0575 is accompanied by an insignificant increase of the heat-transfer intensity. The same figure also shows the textbook equation characterizing heat-transfer intensification in curvilinear pipes and channels [6]:

$$Nu/Nu_{st} = 1 + 3.54d_e/D. \tag{8}$$

It is seen that calculations by Eq. (8) do not reproduce the qualitative features of the flow. Calculations by this equation can give rise to a large error, particularly for curvilinear channels with rectangular-slit cross sections.

The analysis of experimental data on heat transfer in curvilinear channels of rectangular cross section proves the validity of the assumption that if the centrifugal force generated in the cross section of a bent channel is directed along the large dimension of the cross section, and not perpendicularly to it, the effect of heat-transfer intensification is more pronounced. Thus, the use of type-I curvilinear channels is more advisable than that of type-II curvilinear channels.

NOTATION

D, mean diameter of a bend; b, h, cross-sectional width and height; d_e, equivalent diameter; x, length in axial flow direction; Re, Pr, Nu, De = $Re(d_e/D)^{1/2}$, Reynolds, Prandtl, Nusselt, and Dean numbers calculated at mean values typical for a flow; $\theta = T_w/T_f$, temperature factor; T, temperature; $\bar{\alpha}$, α, mean and local heat-transfer coefficients; ξ, hydraulic-resistance coefficient. Indices: e, equivalent; 0, at the entrance; w, mean wall value; f, mean for a flow; f-e, front-end; ex, external; in, internal, L, laminar; T, turbulent; st, straight; I, II, first and second types of channels.

LITERATURE CITED

1. Y. Mori, Y. Uchida, and T. Ukon, Heat and Mass Transfer, 14, No. 11 (1971).
2. A. I. Butuzov, M. K. Bezrodnyi, and M. M. Pustovit, Izv. Vyssh. Uchebn. Zaved., Énerget., No. 11 (1974).
3. D. A. Nusupbekova and B. P. Ustimenko, "A study of hydrodynamics and heat transfer in a planar curvilinear channel," in: Heat and Mass Transfer [in Russian], Vol. 1, Énergiya, Moscow (1968), p. 566.
4. O. A. Gerashchenko and V. G. Fedorov, Thermal and Temperature Measurements [in Russian], Naukova Dumka, Kiev (1965).
5. S. S. Kutateladze, Fundamentals of Heat-Transfer Theory [in Russian], Mashgiz, Moscow–Leningrad (1962).
6. Handbook of Heat Technology [in Russian], Vol. 2, Énergiya, Moscow (1976).

BREAKDOWN OF STABILITY OF HEAT- AND MASS-TRANSFER PROCESSES IN CERTAIN GAS–LIQUID SYSTEMS

M. K. Bezrodnyi

UDC 536.27

Using the critical equation for the limiting regimes of a gas–liquid system with independent flow rate of the gaseous phase, experimental results on the stability of a two-phase mixture are generalized to thermosiphons.

The simultaneous motion of liquid and gas in equipment for different purposes is characterized by an interaction at the boundary of the phases. The characteristics of this interaction, the conditions of exchange of different regimes of motion, the patterns of the flow regimes, etc. have been investigated in [1-4]. In a large number of gas–liquid systems used in practice, it is possible to single out systems with independent flow rate of the gaseous phase and a dynamic two-phase layer [4]. Such systems are encountered in various types of bubbling equipment. Along with the horizontal positioning of the gas-permeable distributor surface (Fig. 1a), systems with vertical surface of the blowing may also by used (Fig. 1b). Closed two-phase thermosiphons with lateral heat supply are a particular case of such systems. The characteristics of the transfer processes in such systems may be significantly different from those in the systems shown in Fig. 1a; this is due to the change in the direction of motion of the phases in relation to the surface of the blowing. At the same time, some useful results may be obtained from the investigation of these processes for individual positions and also from the analysis of well-known experimental results.

We consider a dynamic gas–liquid system in a gravitational field and consisting of two characteristic regions with discrete gaseous and liquid phases, respectively. In order to describe such a system we must set up a system of differential equations describing the transfer processes in the above two regions. The corresponding system of dimensionless groups can be found either directly from this system of equations or from a joint analysis of critical equations obtained for the description of the processes in separate regions of the two-phase flow (the dynamic two-phase layer and the gas flow with liquid drops). In [5], the system of dimensionless groups describing the process of fractionalization and the removal of liquid-drop moisture from the dynamic two-phase layer is derived from the equations of the motion of the vapor–liquid flow, the fractionation of the liquid, the motion of the drop in the vertical flow, and the Laplace and Clausius–Clapeyron equations describing self-evaporation of the

Kiev Polytechnic Institute. Translated from Inzhenerno-Fizicheskii Zhurnal, Vol. 34, No. 6, pp. 1001-1006, June, 1978. Original article submitted May 27, 1977.

